文章编号：1672-9897(2006)04-0001-09

Testing a model scramjet with fuel supplying in hypersonic pulsed wind tunnel

GOONKO Y P, ZVEGINTSEV V I, MAZHUL I I, KHARITONOV A M
(Institute of Theoretical and Applied Mechanics (ITAM), Siberian Branch of Russian Academy of Sciences, Novosibirsk, 630090, Russia)

Abstract: The paper presents results of a scramjet model test in a hypersonic pulsed adiabatic-compression wind tunnel AT-303 recently put into operation at ITAM. The model was tested at Mach number $M_\infty \approx 8$, duration of runs was $\tau = 50 \sim 60$ms, and a wide Reynolds number range of $Re_{1\infty} = 2.7 \times 10^6 \sim 4.0 \times 10^7$ with boundary layer on the model surfaces developing naturally. Due to the model with fuel supply, the gaseous hydrogen was injected into the combustion chamber at air-to-fuel factors exceeding the stoichiometric ratio. The flow conditions sufficient for self-ignition of the hydrogen were provided. Lengthwise pressure and heat flux distribution along the inlet wedge ramp and along the whole engine duct were measured. The obtained results were compared to data of testing the same model in a hot-shot wind-tunnel IT-302M at $M_\infty \approx 6$ and 8, $\tau = 100 \sim 120$ms, $Re_{1\infty} = (1.3 \sim 1.8) \times 10^6$, with boundary layer tripping on the surfaces of the inlet ramp and side compression wedges. It was demonstrated that the flow patterns of the same type developed in the model engine during testing in both the wind-tunnels. Immediately on starting of a wind-tunnel, a supersonic flow pattern formed in the inlet and downstream in the engine duct. After hydrogen injecting, firstly, a combustion flow pattern developed in the combustion chamber with the flow velocity being supersonic on average. After this flow pattern transformed into a flow pattern with thermal chocking at the combustion chamber exit and with a pseudo-shock wave developing in the inlet diffuser. The satisfactory agreement of flow characteristics of the inlet and the engine duct measured in both the wind-tunnels was obtained.

Key words: scramjet; hypersonic pulsed wind tunnel; engine test

高超声速脉冲风洞中带燃料的超燃冲压发动机模型试验

古 科,泽维金茨耶夫,马祖尔,克耐里托诺夫
(俄罗斯科学院西伯利亚分院理论与应用力学研究所,新西伯利亚 630090)

摘要:给出了在ITAM最近投入使用的高超声速脉冲绝热压缩风洞AT-303中进行超燃冲压发动机模型实验的结果。实验马赫数 $M_\infty \approx 8$, 运行时间 $\tau = 50 \sim 60$ms,雷诺数范围 $Re_{1\infty} = 2.7 \times 10^6 \sim 4.0 \times 10^7$,模型表面的边界层自然转捩。在实验中,模型中有燃料供给:把气态氢以超过化学量比率的空气燃料因子注入到燃烧室。提供了足以发生氢燃料自点燃的流动条件。测量了沿进气道楔型压缩面和整个发动机通道上的纵向压力和热流分布。所获数据与同一模型在热射流风洞IT-302M(实验马赫数 $M_\infty \approx 6,8$,运行时间 $\tau = 100 \sim 120$ms,雷诺数范围 $Re_{1\infty} = (1.3 \sim$

* **Received date**: 2006-08-07; Revised date: 2006-08-30
Author biography: GOONKO Y P(1942 -),male, born in Russia, Dr. of ITAM.

1.8)×10⁶,进气道压缩面和侧压缩面进行了边界层转捩)。结果表明:实验模型发动机在两座风洞中进行实验所获得的流态类型相同。发动机刚刚启动时,在进气道入口及其下游的发动机通道内形成超声速流。注入氢后,首先在燃烧室内形成平均流速是超声速的燃烧流动。之后,在燃烧室出口出现热拥塞现象、在进气道扩压段产生伪激波流态。在两座风洞中进行了进气道和发动机通道的流动特征试验,获得了令人满意的结果。

关键词:超燃冲压发动机;高超声速脉冲风洞;发动机试验

中图分类号:V211.7; V235.21 **文献标识码**: A

Basic nomenclature

Free stream parameters:

M_∞ = Mach number

$Re_{1\infty}$ = unit Reynolds number per meter, 1/m

V_∞ = velocity, m/s

ρ_∞ = density, kg/m^3

p_∞ = static pressure, N/m^2

$P_{0\infty}$ = total pressure, N/m^2

$T_{0\infty}$ = total temperature, K

τ = time, ms

θ = angle of compression wedge, degree

χ = sweep angle of wedge-ramp leading edge, degree

A_0 = reference (frontal) area of inlet, m^2

A_∞ = cross-sectional area of free airstream captured by inlet, m^2

A_e = nozzle exit area, m^2

φ = flow rate factor of inlet, $\varphi = A_\infty / A_0$

$\dot{m}_{air}$ = flow rate of airstream $\dot{m}_{air} = \rho_\infty V_\infty \varphi A_0$

$\dot{m}_{H2}$ = flow rate of fuel (gaseous hydrogen)

α = air-to-fuel ratio $\alpha = \dot{m}_{air}/\dot{m}_{H2}$

$\bar{p}$ = relative static pressure, $\bar{p} = p/p_\infty$

q_w = local heat flux through surface, J/(m^2·s)

Cq_w = heat flux referred to specific kinetic energy of free-stream, $Cq_w = q_w/(V_\infty \rho_\infty V_\infty^2/2)$

0 Introduction

One of the major problems, whose solution determines the prospective of creation of hypersonic flying vehicles powered by air-breathing engines, is the development of scramjet-the ramjet engine with fuel injection into a supersonic flow in a combustion chamber. The idea of creation of the scramjet was put forward and substantiated by E. C. Schetinkov in Russia in 1957, and abroad by Dagger, Weber, Jamison, and Ferri at the end of 1950s and early 1960s; further, this concept was developed by many other researchers (see, for example, present-day survey of works on scramjet development and investigations in [1]). Today the principal pathways and tasks for creation of the scramjet are well known, and many research works have been carried out in all possible directions. However, gas-dynamic phenomenon, which take place in flows in hypersonic inlets and in engine ducts with combustion, and intensive heat exchange are still studied insufficiently, because of their complexity, diversity and interdependence. It especially concerns scramjets with three-dimensional inlets, where flows are complicated because of spatial interaction of shock waves with each other and with the boundary layer. One of the most important experimental methods of studying the ramjet/scramjet is testing of model engines in hypersonic wind-tunnels with supply and combustion of different fuels. Although a number of wind-tunnel experiments with scramjets are known (see Ref.[1]), each of them is unique in its own way and such investigations are still always demanded.

Results on testing a model scramjet with a three-dimensional inlet, carried out in a hypersonic pulsed adiabatic-compression wind-tunnel AT-303, are presented in this paper. The general view of the tested configuration is shown in Figure 1. Previous experiments with the engine were carried in a hot-shot wind-tunnel IT-302M at Mach numbers $M_\infty = 6$ and 8[2-4], in both modes with supplying and combustion of gaseous hydrogen and without fuel supplying, and in a blow-down wind-tunnel T-313 at $M_\infty = 4$ and 6 without fuel supplying. Both the wind-tunnels are based at ITAM; the AT-303 is recently put into operation at ITAM. One of the aims of this research (see Ref. [2]) was to obtain experimental data for a generic three-dimensional scramjet configuration, which would be representative enough to determine and to confirm the capabilities of numerical computations of the aero-propulsive characteristics for hypersonic airbreathing vehicles of complex configurations. At the same time the tested configuration should be

rather simple and convenient for computations to be compared with controllable experimental data. Accordingly, for testing in wind-tunnels at ITAM, a model scramjet was developed with a three-dimensional inlet having side compression wedges analogous to inlets of NASA Langley[5~7] and CIAM[8]. Model parameters were chosen so that both the inlet and the engine itself were workable under test conditions, but the objective of reaching a higher efficiency as compared to other types of inlets or scramjets was not pursued therewith.

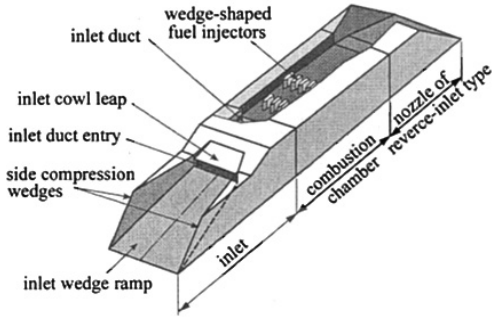

Fig. 1　General view of scramjet model

图 1　超燃冲压发动机模型

The data concerning the pulsed adiabatic-compression wind-tunnel AT-303 are presented in Ref. [9]. This facility provides flow test conditions with high Reynolds numbers close to those full-scale ones possible for scramjet-powered vehicles. Results of the first testing of the said model scramjet with supplying and combustion of the gaseous hydrogen in this wind-tunnel are published in papers [10, 11]. Comparative discussion of the results obtained in testing the model in both the pulsed wind-tunnels IT-302M and AT-303 are given below.

1　Model arrangement

General arrangement and overall sizes of the model are presented in Figure 2. The model was assembled of modular sections so that experiments with the complete scramjet model (inlet + combustor + nozzle) could be performed and the inlet alone could be tested.

The inlet has an upswept wedge ramp, which provides two-dimensional compression of an inlet-captured airstream in a vertical plane, and two side swept-back wedges for lateral compression of this airstream. A cowl of inlet is made with a lip inflected under an angle $\theta_{cl} = 9°$ for the reason of conditions of inlet starting at the least Mach number in the examined range, namely $M_\infty = 4$ in T-313[2-4]. Cross-sectional areas of the engine duct are designed so that the fuel injection into the combustion chamber should occur at a supersonic flow at its entrance. The cross-sections of the inlet internal duct and of the combustion chamber are rectangular. The combustion chamber begins from a stepped extension which follows the inlet diffuser ($x = 400$mm), it has a segment with a constant cross-sectional area (A_{ch} = const up to $x = 555$mm) and a next 2°-diverging segment extended up to the exit of the combustion chamber ($x = 715$mm). The overall increase in cross-sectional area in the inlet diffuser and at the step was chosen so that to avoid the influence of the thermal chocking of the combustion chamber on the flow at the inlet entry during the testing of the complete model in the combustion mode. The nozzle has flat walls, it is designed in a simplest manner as a "reverse" inlet, and side rearmost edges of its exit are oblique. The nozzle provides the exhaust jet expansion in both vertical and horizontal transversal directions.

In the segment of the combustion chamber with constant area of cross-section, two rows of vertical struts with a wedge-like profile are installed for the gaseous hydrogen injection, as one can see in Figure 2. The hydrogen is injected through holes on strut wedges at angles of 65° ~ 75° towards the airflow and under an overcritical pressure difference. Total area of the injection holes provides the supply of 55.5% of fuel through the firststrut-injectors and 45.5% of fuel through the second ones.

The tested model was equipped with gauges to measure the pressure and heat flux distribution. Static pressure was measured in the plane of symmetry of the model ($z = 0$) along the inlet ramp and on the lower and upper surfaces of the inlet and engine duct. Heat fluxes were measured in a lengthwise plane shifted by $z = 20$mm from the plane of symmetry. First taps p_1 and h_1 for pressure and heat flux measurement were located at $x = 105$mm downstream from the leading edge of the inlet ramp wedge. Two rakes with three probes for measurement of local pitot pressure were also installed in the combustion chamber in front of the first fuel-injection struts and behind the second ones.

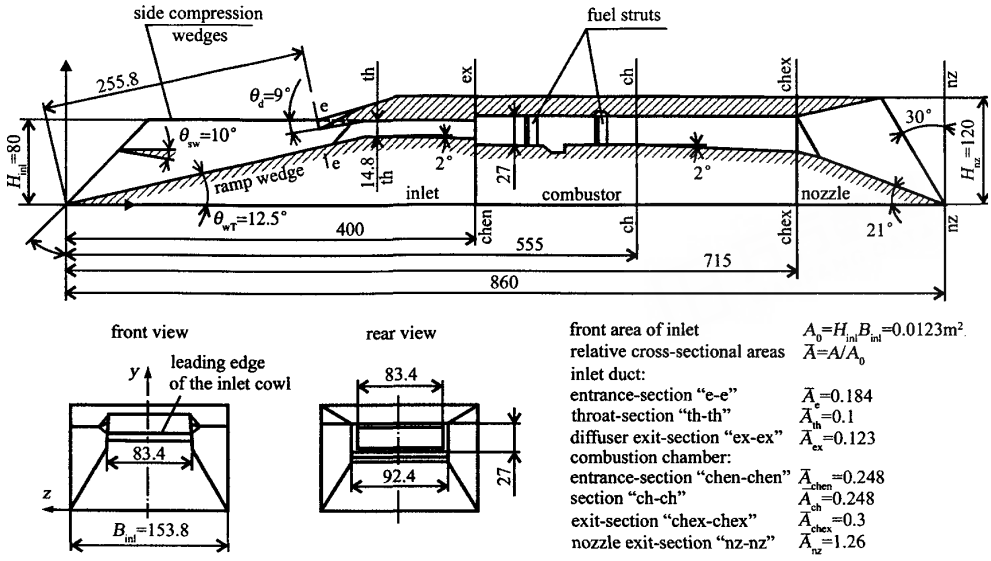

Fig.2 Arrangement and overall dimensions of model scramjet

图 2 超燃冲压发动机模型布局和尺寸图

Small-scale fast-response pressure gauges of an inductive type were used for pressure measurement. They were mounted inside the model in special hermetic containers at 40 ~ 150 mm from measuring holes. According to the calibration data, the basic error of pressure measurement, taking into account the metering system, was 0.2% ~ 1% of the nominal values rated at 10 to 300kPa. As for quasi-steadied pressure values determined and averaged over typical time intervals, the error was about 5% for testing without combustion and 10% ~ 12% for testing in the combustion mode. Heat fluxes were measured with the use of calorimetric gauges developed at ITAM. The response time of heat gauges was about 2.5ms, likely error in temperature measurement was less than 3%, and the error of heat-flux reconstruction was about 10%.

2 Test conditions

Testing in the hot-shot wind-tunnel IT-302M was carried out at $M_\infty = 6$ when a contoured nozzle with a 300mm exit diameter was installed and at $M_\infty = 8$ with a 330mm conical nozzle. The wind-tunnel operates in a regime with pressure stabilization in a discharge plenum chamber. During a run, a quasi-steady flow with near constant parameters in the test section forms in 20 ~ 50ms after the wind-tunnel starting and lasted up to 100 ~ 135ms. The flow parameters in two test series was ranged as following:

$M_\infty = 5.6 \sim 5.8$, $P_{0\infty} = (19.8 \sim 68.0) \times 10^5 N/m^2$, $T_{0\infty} = 1300 \sim 1730K$, $Re_{1\infty} = (1.9 \sim 2.5) \times 10^6$;

$M_\infty = 7.71 \sim 7.89$, $P_{0\infty} = (54.0 \sim 117.6) \times 10^5 N/m^2$, $T_{0\infty} = 2270 \sim 2320K$, $Re_{1\infty} = (1.2 \sim 1.4) \times 10^6$.

It should be noted that, since the Reynolds numbers in IT-302M were low, the test data for the model under consideration were obtained with tripping of the boundary layer over the inlet compression wedges. Namely these data are discussed below.

The regime of exploitation realized in AT-303 for $M_\infty = 8$ at present time, provides the quasi-steady operating flow with near constant Mach number and with such little-varying quantities as, for example, $p_\infty / P_{0\infty}$, although absolute values of the total and static pressures or temperature as well as Reynolds number vary in time. The operating flow is settled in 15 ~ 20ms after the wind-tunnel starting, by the moment when the total pressure reaches its highest value $(P_{0\infty})_{max}$, and lasts for next 30 ~ 40ms. Some features of the testing in AT-303 are discussed in [11]. Typical flow parameters corresponding to pressure $(P_{0\infty})_{max}$ for a series of tests are:

$M_\infty = 7.76 \sim 8.2$, $P_{0\infty} = (38.4 \sim 418) \times 10^5 N/m^2$, $T_{0\infty} = 1140 \sim 1430K$, and $Re_{1\infty} = 2.7 \times 10^6 \sim 4.0 \times 10^7$.

The model was installed in wind-tunnels so that the leading edge of its inlet was located upstream of the nozzle exit by $L_{le} = 365mm$ for IT-302M and $L_{le} = (100 \pm 2)mm$ for AT-303, i.e., the model forebody was fitted into the Mach-line rhombus corresponding to the diameter of the flow core at the wind-tunnel nozzle exit for taking into account the boundary-layer thickness. For both the wind-tunnels, parameters determined for the said flow core were taken as parameters of free stream blowing onto the model.

3 Inlet characteristics

The inlet characteristics in AT-303 were obtained in a range of Reynolds numbers $Re_{1\infty} = 2.7 \times 10^6 \sim 3.8 \times 10^7$. From analysis of time dependences of pressure measured in the inlet, which was carried out in [11], it follows that, with settling the operating-flow in 15 ~ 20ms after the wind-tunnel starting, the $p_i/P_{0\infty}$ values are thereabout constant during time intervals from 30 to 10 ms, depending on a pressure tap under consideration p_i ($i = 1 \cdots 13$). This specifies the model flow pattern as quasi-steadied. Relative pressure levels at all the taps correspond to supersonic flow in the inlet duct. 50 ~ 60ms after the wind-tunnel starting, pressure in the inlet duct sharply falls, which indicates that the supersonic flow pattern in the model begins to break down. Lengthwise distribution of relative pressure in the inlet (on the wedge ramp and on the lower wall of the internal duct) is presented in Figure 3. Values ($\bar{p}_i = p_i/p_\infty$) plotted for every pressure measure tap in this figure correspond to the relative values $p_i/P_{0\infty}$ averaged over the lifetime interval of the quasi-steady flow in the inlet duct. Presented test data are obtained for a set runs with different values of $(P_{0\infty})_{max}$ and Reynolds number $Re_{1\infty}$.

It should be noted the following flow features, which were identified in testing the scramjet model in IT-302M[2-4]. The inlet ramp and side compression wedges generate shock waves propagating downstream along corners between the wedges and being glancing with respect to the flat compression surfaces. These shock waves induce oblique boundary-layer separations - their separation lines emanate from the corner apexes, they are swept and develop in different ways depending on the boundary-layer state. Oblique shock waves arise along the separation lines and helical curls develop in the separation zones. Wedge-generated shock waves and the related induced separation zones propagating over the ramp wedge and towards the plane of symmetry of the inlet collide with each other before reaching the inlet-duct entrance. As a result, a central complex-separation zone forms over the ramp wedge surface. The tracks of the separation-induced oblique shock waves emanating from the beginning of the central separation zone in the plane of symmetry, respectively for the laminar and turbulent boundary layers, are shown in Figure 3 by data obtained in testing the model in IT-302M at $M_\infty = 8$. Judging from these data, the flow perturbations related to the formation of the oblique separations for the laminar boundary layer on the ramp wedge manifest themselves, in the plane of symmetry, near the pressure tap p_2. The pressure at the tap p_1 is not affected by these flow perturbations. At this station, the level of measured pressure $\bar{p}_1$ compares well with the level estimated for an oblique shock wave formed by the ramp wedge under the assumption that the adiabatic exponent is constant ($\gamma = const = 1.4$). A character of the pressure distribution in the inlet duct is determined by the impact of shock waves forming in the vicinity of the external-compression wedges and subsequently penetrating into the duct, of new shock waves generated by the inlet cowl lip, of shock waves reflected from the internal-duct walls, and by local boundary-layer separations. At the highest $Re_{1\infty} = 3.8 \times 10^7$, the pressure level in the inlet duct behind the entrance cross section is generally 1.2 ~ 1.6 times less than that measured at lower Reynolds numbers $Re_{1\infty} \leqslant 2.7 \times 10^7$. The character of the lengthwise pressure distribution with a peak behind the inlet throat and the level of pressure obtained in the latter case agree well with those obtained in the tests of the model in IT-302M at $M_\infty = 7.9$ and $Re_{1\infty} = 1.3 \times 10^6$ with boundary layer tripping; the data obtained in IT-302M are also shown in Figure 3 for comparison.

The lengthwise distributions of normalized heat-fluxes Cq_w in the inlet are shown in Figure 4. The heat-fluxes are measured in the longitudinal plane $z = 20mm$; in this

case, the flow perturbations induced by the oblique boundary-layer separations manifest themselves closer to the ramp-wedge leading edge rather than in the plane of symmetry. The tracks of the separation-induced oblique shock waves for the laminar and turbulent boundary layers, according to the IT-302M data[15-16], are shown in Figure 4 for the shifted plane $z = 20$mm; only data taken at the tap h_1 are seen to not be affected by these flow perturbations. The heat flux coefficient Cq_w determined experimentally at this tap in the IT-302M tests with boundary layer tripping agrees with an estimate obtained for the turbulent boundary layer in [15-16] (see Figure 4, curve 1). Analogously to [15-16], the reduced heat fluxes were also calculated for the test conditions in AT-303. Figure 4 shows the curves $Cq_w(x)$ predicted for the turbulent (curve 2) and laminar (curve 4) boundary layers under the lowest Reynolds number $Re_{1\infty} = 2.7 \times 10^6$ and for the turbulent (curve 3) boundary layer under the highest Reynolds number $Re_{1\infty} = 3.8 \times 10^7$. It is seen that, for $Re_{1\infty} \geqslant 5.4 \times 10^6$, the heat flux measured at the tap h_1 agrees with the heat flux predicted for the turbulent boundary layer, whereas at $Re_{1\infty} = 2.7 \times 10^6$ it agrees better with the value predicted for the laminar boundary layer. In the latter case, the measured heat flux increases in the downstream direction between taps h_1 and h_2 and at the tap h_2 it already becomes consistent with the estimate obtained for the turbulent boundary layer. This gives us grounds to believe that the boundary layer on the inlet ramp wedge was transitional at $Re_{1\infty} = 2.7 \times 10^6$—laminar at $x = 105$mm (h_1 tap) and turbulent at $x = 163.6$mm (h_2 tap). The data obtained for $Re_{1\infty} \geqslant 5.4 \times 10^6$ show that the transition of the boundary layer to the turbulent state occurred at $x < 105$mm. The lengthwise heat-flux distributions obtained in AT-303 tests at $Re_{1\infty} \geqslant 5.4 \times 10^6$ display a near-constant level of heat fluxes in the flow region between the taps h_1 and h_2, a maximum in front of the internal-duct entrance, and a minimum at the throat. This character is analogous to the one previously observed in IT-302M, although the level of heat fluxes in the latter case is higher. That can be explained by a higher total temperature in IT-302M tests and by the fact that the turbulent boundary layer in this wind-tunnel was obtained with tripping, whereas the predominantly turbulent boundary layer in the AT-303 tests developed naturally.

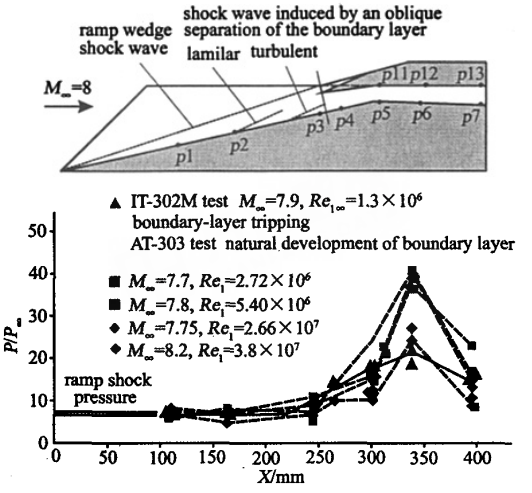

Fig.3 Lengthwise pressure distribution in inlet

图 3 进气道内纵向压力分布

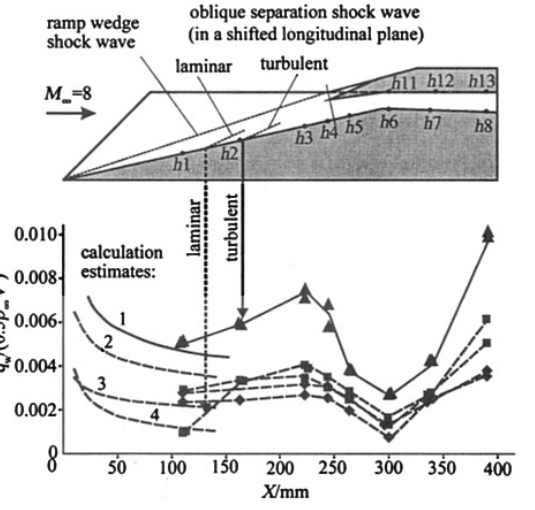

Fig.4 Lengthwise heat-flux distribution in inlet (notations see in Fig.3 and in the text)

图 4 进气道内纵向热流分布

4 Characteristics of model scramjet

The tests on determination of characteristics of the whole model scramjet were performed at high Reynolds numbers, $Re_{1\infty} = 3.4 \sim 4.0 \times 10^7$; the model was tested both in regimes with out fuel supplying and with hydrogen combustion. The gaseous hydrogen was supplied under various initial fuel-tank pressures, $P_{0H_2} = 45 \sim 12.5 \times 10^5$Pa. A delay of fuel valve opening was chosen so that the hydro-

gen entered the combustion chamber at the instant when the quasi-steady flow pattern in the inlet had already set. In every case the hydrogen self-ignited and its burning occurred. The hydrogen flow rate was estimated by the change of the pressure measured in the fuel tank; considering the short durations of a run, the flow rate of hydrogen decreased almost linearly in time. The mass flow rate $\bar{m}_{air}$ of the airstream captured by the inlet was not measured; instead, this rate was estimated using an inlet flow-rate factor $\varphi = 0.52$ determined at $M_\infty = 8$ in the IT-302M tests (with boundary-layer tripping). It can be assumed that in the AT-303 tests this factor could be somewhat higher because the boundary layer on the compression wedges was thinner due to its natural development and the $Re_{1\infty}$ numbers were higher by one order of magnitude.

The time dependence $\dot{m}_{air}(\tau)$ of the flow rate of airstream captured by the inlet and passing through the engine duct is determined by varying of the flux $\rho_\infty V_\infty$; i.e., it closely follows to that of the total pressure $P_{0\infty}(t)$. The value $\dot{m}_{air}$ attains its maximum in 15 ~ 17ms after the wind-tunnel starting, then, the flow rate $\dot{m}_{air}$ of the air decreases more rapidly than the flow rate $\dot{m}_{H_2}$ of the hydrogen. Accordingly, the air-to-fuel factor $\alpha = \dot{m}_{air}/\dot{m}_{H_2}$ decreases during the test from near the maximum of $\alpha = 7.6 \sim 8.7$ to $\alpha \cong 3.2$ by the time when the flow regime in the model suffers breakdown about 55 ms after the wind-tunnel starting.

Data of pressure measurement depending on time is evident[11] that there are typical time intervals of change in the pressure level in the combustion chamber. The hydrogen ignites in 15 ms after the wind-tunnel starting. During 8 ~ 10 ms before its ignition, pressure in the combustion chamber attains very nearly a level, which corresponds to the quasi-steady flow pattern in testing without fuel supplying. Very simple estimates of engine airflow parameters were made based on measurement of static pressure on the duct walls and pitot pressure with the rakes installed in the combustion chamber. The estimated flow was assumed one-dimensional. In particularly, for testing at $M_\infty = 8.2$, $(P_{0\infty})_{max} = 4.18 \times 10^7$Pa, $T_{0\infty} = 1140$K, $P_{0H_2} = 2 \times 10^6$Pa, it was gained that of the flow velocity at the entrance of the combustion chamber corresponds to a Mach number $M_{ch} \approx 2.2$, the static temperature of the air is about 1070 K, at that, the air-to-fuel ratio increases to this moment from $\alpha = 4.1$ up to 7.7, i.e. up to the value closing to the mentioned maximum value. With the hydrogen igniting, the pressure at the combustion chamber entrance rises at once, after that its level is approximately constant during 10 ~ 15ms. From this moment, the pressure in the combustion chamber gradually increases and this increase extends upstream into the inlet diffuser and further towards the inlet throat. The pressure perturbation attains the inlet throat in 45ms later but does not go out ahead of the inlet duct entrance. The pressure in the combustion chamber increases till the moment about of 40 ms, after that a pressure level stays roughly constant in a time interval about 10ms. 55ms later, the pressure perturbation goes ahead out of the inlet-duct entrance, the pressure in the engine duct increases again, then sharply falls. That manifests a break down of the flow regime in the engine; this flow destruction is following by a terminate flow pattern in the inlet, apparently, with a bow shock at its entrance. Note the break down of the combustion flow pattern in the model engine takes place at the same time as the quasi-steady flow pattern terminates in the inlet tested alone, as said above.

The lengthwise pressure distribution along the inlet ramp wedge and the lower wall of the engine flow path both in combustion and no combustion modes are presented in Figure 5. Relative pressure values $\bar{p}$ averaged in above mentioned typical intervals are plotted. Figure 5a presents the pressure change at the time just after the wind-tunnel starting. In a time interval of 10 ~ 15ms after the starting moment and before the hydrogen ignition, pressure in the combustion chamber corresponds to a pressure level in testing with no fuel supplying. In a time interval of 15 ~ 25ms the pressure level in the combustion chamber is $\bar{p}_{ch} = 23 \sim 45$ at the first fuel-injection struts and $\bar{p}_{ch} = 38 \sim 50$ at the second one. At that, the pressure level in the inlet corresponds to that in testing with no fuel supplying. In a time interval of 27 ~ 45ms the pressure in the combustion chamber and in the inlet diffuser gradually increases but the pressure perturbation does not go out ahead of the inlet duct entrance. The pressure level in the combustion chamber at

the end of this time interval (40 ~ 45ms, Figure 5b) is $\bar{p}_{ch}$ = 30 ~ 67 at the first fuel-injection struts and $\bar{p}_{ch}$ = 35 ~ 60 at the second one. In both combustion flow regimes pressure drops at the beginning of the diverging segment of the combustion chamber (x = 555mm), which indicates that the combustion terminates here.

The said combustion-flow patterns, the initial one without pressure increasing in the inlet diffuser (10 ~ 15ms) and the posterior one with pressure in diffuser, which increases upstream up to the inlet throat (40 ~ 45ms), as well as the characters of pressure distribution along the whole model duct in these regimes, are analogous to those obtained in testing the model scramjet in IT-302M[2-3]. Identification of these flow patterns was supported by comparison of measured pressure levels to estimates of pressure change in the inlet diffuser and in the combustion chamber with heat addition due to fuel burning, calculated in one-dimensional flow approximation. It was concluded from the estimates that, just after the hydrogen ignition, a flow velocity was supersonic on average, as it was exemplified. Then, critical conditions of flow choking with $M_{ch} \approx 1.0$ arose near the exit from the combustion chamber segment with constant area of cross-section, and the combustion flow regime with a precede pseudo-shock wave in the inlet diffuser developed. It is a regime with heat addition behind the pseudo - shock wave in a short

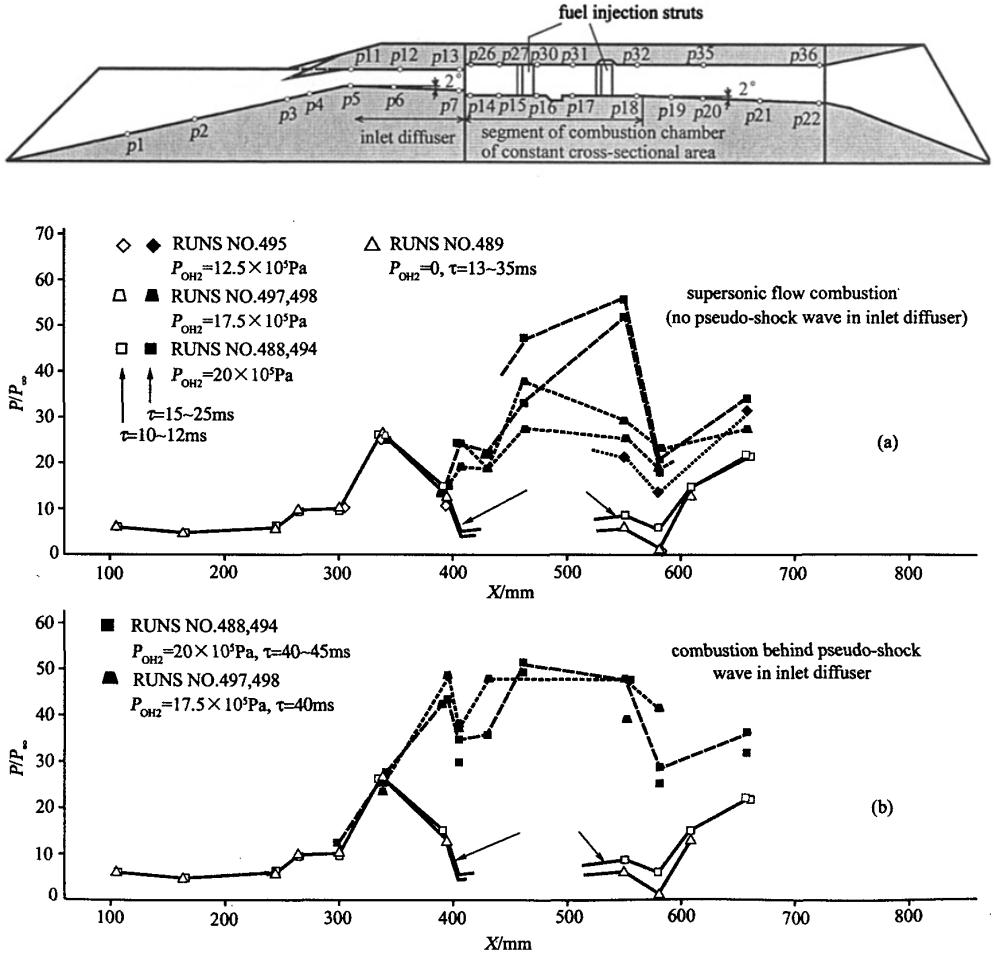

Fig.5 Lengthwise pressure distribution along model scramjet flow path

图5 沿超燃冲压发动机模型流道上的纵向压力分布

channel[12], which is also named a pseudo-shock regime of combustion[13]. The correspondence of the flow properties with combustion in the model engine duct in IT-302M and AT-303 permits us to suppose that both the combustion-flow regimes are identical.

On the whole, the results on comparative study of the considered model scramjet in both the pulsed wind-tunnels, in the hot-shot IT-302M and in AT-303 of adiabatic compression, with higher parameters of operating flow in AT-303 but with the run duration somewhat less than that of IT-302M, prove the same time-depending properties of developing the gas dynamic processes in the engine that were previously determined in tests of axisymmetric ramjet models in hot-shot wind-tunnels IT-301 and IT-302 based at ITAM[14-15]. Processes of development and transformation of the flow patterns in the combustion mode are analogous in all these cases. So that the time-depending properties of developing gasdynamic processes at testing the hypersonic engine models in the new pulsed wind-tunnel are quite suitable for studying of scramjet characteristics.

References:

[1] CURRAN E T, MURTHY S N B, Editors. Scramjet propulsion [J]. Progress in astronautics and aeronautics, 2000, 189.

[2] CHALOT F, ROSTAND Ph, PERRIER P, et al. Validation of global aero-propulsive characteristics of integrated configurations [R]. AIAA Paper 98 ~ 1624, 1998.

[3] ADAMOV N, GOONKO Y, KHARITONOV A, et al. Study on drag-thrust forces of a scramjet model in blow-down and hot-shot wind tunnels [C]. International Conference on the Methods of Aerophysical Research (ICMAR'98), Novosibirsk, Russia, Part 3, 1998. P. 3 ~ 9. Published by ITAM.

[4] GOONKO Y P, MAZHUL I I, LATYPOV A F, et al. Structure of flow over a hypersonic inlet with side compression wedges [J]. AIAA Journal, 2003, 41(3):436 ~ 447.

[5] HENRY J R, ANDERSON G Y. Design consideration for the airframe-integrated scramjet. Proceedings of the first international symposium on air-breathing engines. // GURYLEV V G, STARUKHIN V P, and KUKANOVA N I. Inlets for hypersonic air-breathing engines. Survey of ONTI TsAGI. 1977 (522).

[6] TREXLER C A. Performance of an inlet for an integrated scramjet concept [J]. J. of Aircraft. 1974(9):588 ~ 591.

[7] HUNT J L, JOHNSTON P J, CUBBAGE J M. Hypersonic air-breathing missile concepts under study at langley [R]. AIAA Paper 82-316, 1982.

[8] VINOGRADOV V A, STEPANOV V A, ALEXANDROVICH E V. Numerical and experimental investigation of an airframe-integrated inlet for high velocities [R]. AIAA Paper 89-2679, 1989.

[9] KHARITONOV A M, ZVEGINTSEV V I, FOMIN V M, et al. New-generation hypersonic adiabatic compression facilities with pressure multipliers // FRANK LU, DAN MARREN. Advanced hypersonic test facilities, Progress in astronautics and aeronautics. 2002,198, AIAA, Reston, Virginia:585 ~ 619.

[10] GOONKO Y P, KHARITINOV A M, MAZHUL I I, et al. Investigation of a scramjet model at hypersonic velocities and high Reynolds numbers [R]. AIAA Paper, 2002-5273. (11th AIAA/AAAF international conference, 29 September ~ 4 October 2002, Orleans, France).

[11] GOONKO Y P, KHARITINOV A M, MAZHUL I I, et al. Wind-tunnel tests of a model scramjet under high Mach and Reynolds numbers [J]. Thermophysics and Aeromechanics, 2003,10(3):315 ~ 337.

[12] SHCHETINKOV E S. Piecewise one-dimensional models for supersonic combustion and pseudo-shock wave in a channel [J]. Combustion, Explosion and Shock Waves. 1973,(4): 473 ~ 482.

[13] TRET'YAKOV P K. Pseudo-shock regime of combustion [J]. Combustion, Explosion and Shock Waves, 1993(6): 33 ~ 38.

[14] BAEV V K, SHUMSKY V V, YAROSLAVTSEV M I. Some methodical aspects of studying gasdynamic models with heat and mass addition in a hot-shot wind tunnel [J]. Combustion, Explosion and Shock Waves. 1987(5):45 ~ 54.

[15] BAEV V K, SHUMSKY V V, YAROSLAVTSEV M I. Study of combustion and heat exchange processes in high enthalpy short duration facilities [A]//Murthy N B and Curran E T, High speed propulsion system, Progress in Astronautics and Aeronautics, 1991,137, AIAA.